

#### 5.2.4.2 Consistency of fragmentation density distribution

The essence of the method of determining the missile's orientation relative to the aircraft according to the density of fragmentation damage is to find the best correspondence between the picture of impact element distribution in the field of virtual warhead cover and the observed density of projectiles on the detected fragments (wreckage) of Boeing 777.

The result is the best fit of the dynamic fragment dispersion model to the damage density distribution model, taking into account the detonation point that connects them.

Most importantly, the Almaz-Antey specialists used the Damage Model as a benchmark for comparison, which takes into account the most important fragments of the roof and top of the port side beyond STA 220.5, characterising not only the actual rear boundary of the fragmentation field, but also being areas of high density of fragmentation damage.<sup>80</sup>

The Almaz-Antey damage model takes into account the damage not only on the fragments presented in the 3D reconstruction, but also on the roof and upper port side fragments that did not make it to the final layout (see paragraph 5.1.2).

The fragmentation damage in the model is an array  $\mathbf{a}$ , which stores the number of penetrations for each of the  $M$  sites that make up the nose of the Boeing 777.

For the Boeing 777 model used, the number of sites  $M = 5,365$ . The array  $\mathbf{a}$ , storing the number of fragmentation impacts in each of the aeroplane's seats, was the reference.

The meaning of the algorithm for solving the problem of determining the conditions of meeting an aircraft with a missile (the orientation of the missile relative to the aircraft at the time of detonation) is as follows. At various points in the region of space (less than  $1 \text{ m}^3$ ), which constitutes the verified detonation point region, the missile's payload is detonated, taking into account the mutual speed of approach to the aircraft with different angles of azimuth  $Az$  and angles of location  $El$ .

For each detonation, the trajectories of each fragment and the points of intersection of these trajectories with the planes that make up the surface of the aircraft are calculated. For each case, the points found are stored in a data array, each element of which represents the number of impacts falling on the area with the number corresponding to the element index. Such arrays are approximations (approximations).

For all the approximations found, error  $E$  is calculated, which quantifies the difference between the approximation array and the benchmark and is used as a criterion for selecting the approximation array that most closely matches the benchmark. The value of error  $E$  for it is the lowest among the values of other approximations.

---

<sup>80</sup> PART 2. Exhibit A.

As a result, the solution to the problem is reduced to a numerical solution to the optimisation problem:

$$E(\mathbf{p}^{\rightarrow*}) \rightarrow \min_{\mathbf{p}^{\rightarrow} \in P} E(\mathbf{p}^{\rightarrow}),$$

where,  $\mathbf{p}^{\rightarrow} \equiv (x, y, z, Az, El)$  is a five-dimensional vector;

$(x, y, z)$  are the Cartesian coordinates of the centre of the SAM system;

$Az$  and  $El$  are the azimuth and the angle of engagement of the SAM system;

$\mathbf{p}^{\rightarrow*} \equiv (x^*, y^*, z^*, Az^*, El^*)$  is the desired solution that gives a minimum to the functional  $E(\mathbf{p}^{\rightarrow})$ .

For the numerical calculations, the following minimisation criterion was chosen:

$$E = \sum_{i=0}^{M-1} |e_i - a_i|$$

where  $M$  is the number of sites (polygonal objects) that make up the surface of the Boeing 777-200 ER aircraft model;

$e$  - array storing the number of penetrations per site according to the simulation results (for each of the approximations);

$a$  - an array storing the number of penetrations per site in the Benchmark - "Damage Models".

The number  $E$  in this criterion corresponds to the number of non-matched faults. The choice of this criterion is due to its obviousness and ease of implementation.

To solve such problems, it is necessary to enumerate many different positions of the warhead and compare them with the reference value. The position of the warhead in space is determined using five parameters: three Cartesian coordinates, elevation angle and azimuth (Figure 5.2.20).

The brute-force method is computationally intensive and time-consuming. For example, it takes about 2 seconds to calculate one explosion.<sup>81</sup> A brute force attack (an ARM with a 2.4 GHz *Intel Xeon E5620* processor) would take about 4 years to compute and would be approximately 60 million variants.

The time required to complete a full search was reduced by performing calculations on the Orpheus-K supercomputer using parallel algorithm.<sup>82</sup>

<sup>81</sup> This figure is obtained by experimental measurements on the Orpheus-K supercomputer.

<sup>82</sup> MPI - *Message Passing Interface* technology was used, which reduced the complete enumeration time for both the coarse and fine mesh to 12 days.

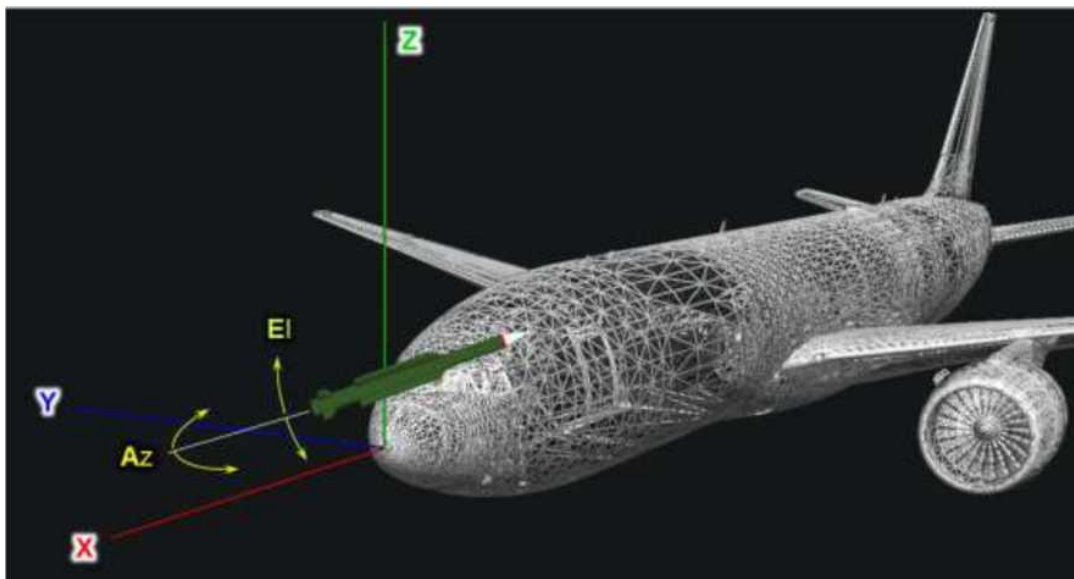


Figure 5.2.20 - Parameters for enumerating SAM position in space: X, Y, Z - position of the centre of the warhead relative to the origin of coordinates; Az, E1 - azimuth and location angle of the missile's longitudinal axis

The calculation was carried out. The range of best results for the spatial position of the missile's warhead relative to the aircraft at the time of detonation at a final missile velocity of 600 to 730 m/s was

Azimuth (Ag, horizontal plane), degrees .....-62... -68  
 Angle of seating (E1, vertical plane), degrees .....20...24

One of the variants resulting from the calculations was used as a baseline for the first phase of the experiment. The calculated vector had values corresponding to the Corporation's version of the 'collision course':

Angles of the SAMS relative to the aircraft: azimuth angle  $-66^\circ$ ; elevation angle  $22^\circ$ ; detonation point coordinates:  $X = 0.5$  m,  $Y = -1.5$  m,  $Z = 1.7$  m; final rocket speed of 720 m/s.<sup>83</sup>

If possible, the results of the calculations should be verified by other available methods.

One of the most acceptable markers, which can be easily checked, is the second window (vent) of the crew commander. Its exact dimensions are given in the DSB Report. There it is also shown that the second window was in the area of maximum fragmentation density and 102 fragmentation injuries were recorded on it.<sup>84</sup>

This area, including the second window, was a kind of reference point for the Dutch experts, using which the experts searched for and verified the rendezvous conditions of the missile by plane.<sup>85</sup>

In order to compare the actual and simulated damage in the second left window

<sup>83</sup> The results of the match with the benchmark were over 96%.

<sup>84</sup> Final Report. Cockpit window left hand side, Figure 34, p.79.

<sup>85</sup> Final Report. Annex X (NLR report). 2.5 Number and density of hits, p.14.

in terms of number and density of damage, simulations were performed for different values of the azimuth (horizontal angle) of the final missile position from the ranges obtained by different specialists:

Missile end state (at time of warhead detonation): angle of location (E1, vertical angle), degrees .....(5)  
Detonation area coordinates, m ..... (0.4; - 1.85, 1.85)  
missile speed, m/s ..... 600

Only the value of the azimuth (the angle between the aircraft and rocket axes) was changed to the fixed values present in the various reports:

azimuth (Az), degrees (-16; -37; -50; -62; -66; -68)

The options were compared using an interactive 'simulated damage' model and an 'actual damage' model of the second left window (102 fragmentation injuries according to the DSB Report).

As noted earlier, the dynamic fragment dispersion model takes into account the different types of fragments: ready-made two types of light fraction (Light) and heavy fraction (Heavy), as well as shell fragments (Shell).<sup>86</sup>

When assessing fragmentation damage to windows, only prefabricated impactors should be considered. This assertion is based on experimental data obtained from in-situ experiments: cockpit transparency, 25mm laminated glass, can only be penetrated by prefabricated (primary) projectiles.<sup>87</sup>

An example simulation for the Azimuth -16° variant is shown in Figure 5.2.21, where the set of areas (polygonal objects) corresponding to the second left window on the Boeing 777 is highlighted in orange on the interactive aircraft model.

A pop-up window indicates the number and types of fragments whose trajectories intersected the areas that make up the surface of the second left-hand cockpit window.

---

<sup>86</sup> Only hull fragments with linear dimensions corresponding to the size of the GGE are counted. Detonation products of 1-3 mm in size and large compartment fragments are not counted.

<sup>87</sup> PART 2. Exhibit B.3.

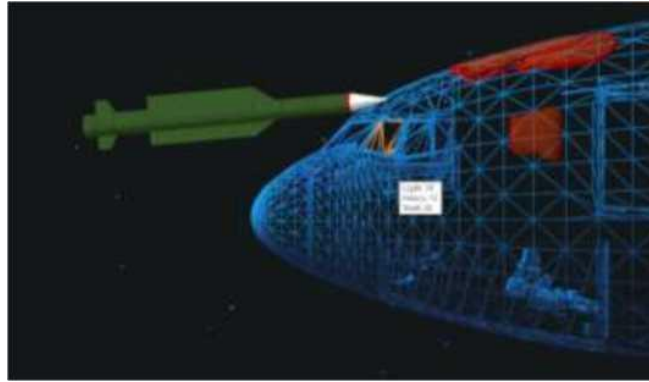


Figure 5.2.21 - Simulation of fragmentation damage to the nose of a Boeing 777 aircraft under Azimuth  $-16^{\circ}$  conditions. The polygonal objects corresponding to the second left window are highlighted in orange on the interactive aircraft model

The simulation results in only 72 splinters in the second window:

Light .....	34	(light fraction projectiles of two types)
Heavy .....	12	(heavy fraction projectiles, "bowtie")
Shell .....	26	(hull splinters)

Accordingly, the simulation results show that only 46 prefabricated projectiles (34+12= 46) could damage the complex multi-layer barrier that is the cabin transparency (window).

The number of simulated damages (46 units) is 2.22 times less than the number actually recorded in the second window (102 units).

Similarly, a comparative analysis of modelled and actual damage for the other variants of the range of possible angles is performed. The results of two more important Azimuth  $-37^{\circ}$  and Azimuth  $-50^{\circ}$  variants characterising the range of missile impact conditions for the aircraft are shown in Figure 5.2.22.

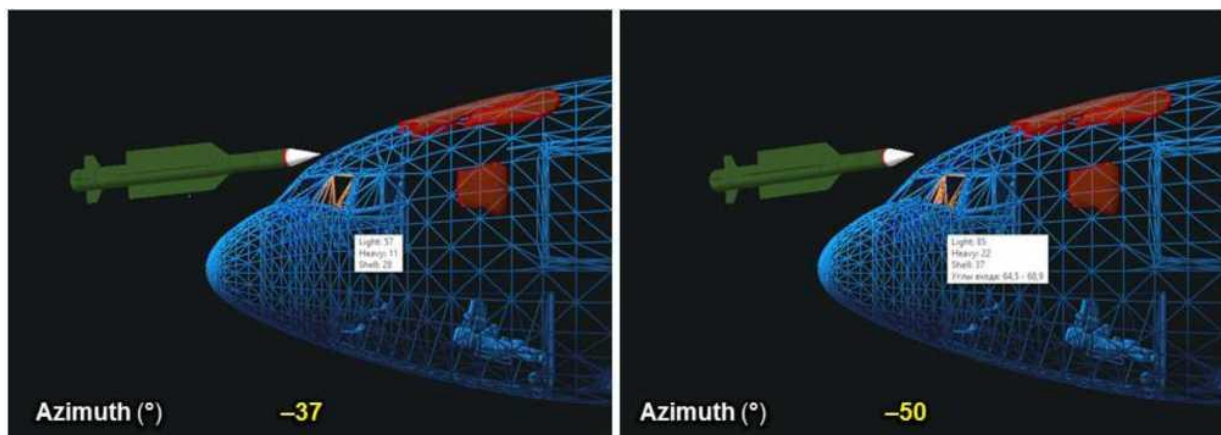


Figure 5.2.22 - Simulation of fragmentation damage to the nose of a Boeing 777 aircraft under Azimuth  $-37^{\circ}$  (left) and Azimuth  $-50^{\circ}$  (right) conditions

A. For "Azimuth  $-37^{\circ}$ " conditions:

up to 96 fragments (Light- 57; Heavy- 11; Shell- 28) can reach the second window;

no more than 68 prefabricated projectiles (57+11= 68) could damage the complex multi-layer barrier that is the cab's transparency (window);

The number of simulated damages (68 units) is 1.5 times less than the number actually recorded in the second window (102 units);

The modelled damage density for Azimuth -37° conditions is 1.5 times lower than the actual damage density and is about 167 punctures per square metre.

B. For "Azimuth -50°" conditions:

The second window only receives up to 144 fragments (Light- 85; Heavy- 22; Shell- 37);

Up to 107 prefabricated projectiles (85+22= 107) could damage the complex multi-layer barrier that is the cab's transparency (window);

The number of modelled damage (107) is comparable to the number of actually recorded damage at the second window (102), and the modelled density is also comparable to the actual values recorded at the second window - about 250 punctures per square metre.

The modelling results for all variants are shown in Figure 5.2.23 as a histogram, from analysis of which the range of acceptable azimuth values is from -50° to -68°, with the best match for -66°.

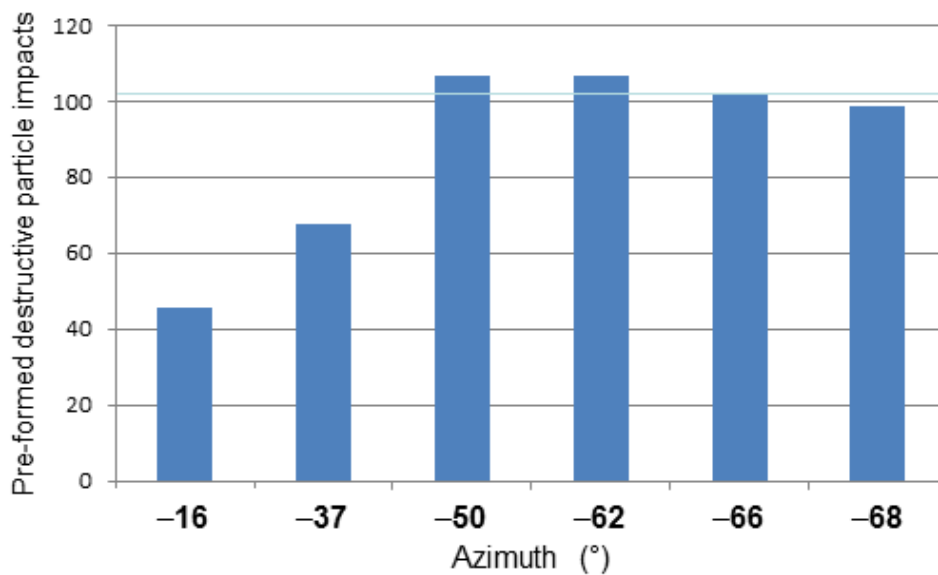


Figure 5.2.23 - Fragmentation damage to the second left window when the missile's warhead is oriented at horizontal angles ranging from -16° to -68°

Similar calculations were made for the other important roof and port top fragments not shown in the final layout.

For example, the upper port side fragment (Figure 5.2.24) shows a high density

of damage at the level of the STA 287.5 and STA 298.5 bulkheads.<sup>88</sup>

The particular importance of this fragment lies in the fact that it is located twice as far from the boundary used in the NLR - STA 220.5 models and more than twice as far from the second left window (STA 164.75- STA 188.5). Taking into account that with distance from the detonation point - the fragmentation field density decreases inversely proportional to the square of the distance ("law of squares"), respectively, if the distance from the detonation point to the outer surface of the aircraft changes by half, the actual density of damage on this surface should change by a factor of four. Taking into account the additional fragments, the range of acceptable azimuth values is from  $-62^{\circ}$  to  $-68^{\circ}$ , and the best match remains for a value of  $-66^{\circ}$ .

A damage model that does not include critical fragments such as the roof of the cockpit, the fragments with the highest density of projectiles is inaccurate.

Numerical experiments have found that areas of higher density have a greater influence on the target function, and accounting for missing roof and port side fragments provides a more accurate simulation.

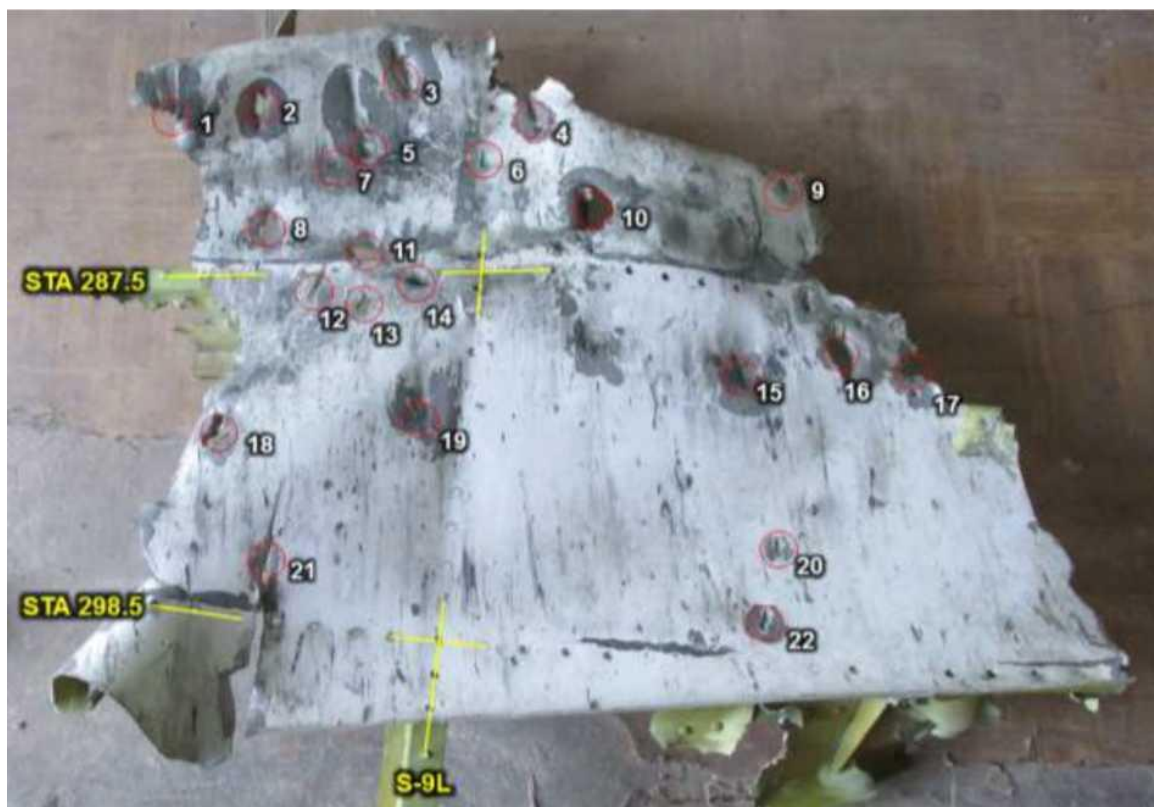


Figure 5.2.24 - Fragment with high density of fragmentation damage not included in final reconstruction and not included in NLR models

It should be noted that, as a result of a comparative analysis of the shielded target situation with damage to the outer hull fragments, elements of the structure of

<sup>88</sup> The fragment was not included in the final reconstruction, but was located in the Netherlands in another room.

the Boeing 777 (MH17) aircraft, it was the field of coverage of the main elements of the nose section of the aircraft and the distribution of the density of fragmentation damage were found to be consistent.

For the range of warhead orientation angles determined by this method ( $-62^\circ$  to  $-68^\circ$ ), the comparison criterion No. 3 (impact density distribution) specified in paragraph 5.1.3 of the Corporation Report is best fulfilled.

---

Thus the consideration of fragments with a high density of fragmentation damage on the roof and upper port side behind the cockpit to the level of STA 287.5-STA 332.5 (not included in the 3D reconstruction and located almost 3 metres beyond the "reference" STA 220.5), significantly affects the credibility of the determination of the missile-aircraft encounter conditions.

The range of best results for the spatial position of the missile's warhead relative to the aircraft at the time of detonation for a final missile velocity of 600 to 730 m/s is  $-62^\circ$  to  $-68^\circ$ .

The destruction of a Boeing 777 aircraft by a BUK missile can only be considered on a "collision course", i.e. at an angle of at least  $-50^\circ$ .

---

### 5.2.4.3 Destruction of aircraft structure by a dense stream of projectiles ("scalpel")

The piercing of an aircraft structure and the mechanical destruction of its compartments is caused by a dense stream of fragments and the resulting shock waves (ballistic waves of fragments in an airborne environment).

The ability to penetrate several successive or combined obstacles is directly related to the velocity of the projectiles, their mass and shape.

Experimental studies conducted show that:

1. Preformed fragments (Figure 5.2.25 below), having a compact shape and greater mass, have a significantly higher penetration.

2) The ballistic wave of fragments of the required intensity is generated only in areas of high density of preassembled projectiles (PDEs). The PGEs themselves must have a large mass and area in order to transmit the maximum impact force momentum to the barrier, which, for a BUK missile, corresponds to fragments of the heavy fraction 9H314M 1-10 ("double-barreled").



Figure 5.2.25 - Comparative linear dimensions and mass of hull fragments (top) and 9H314M heavy fraction preformed fragments 1-10 "doublet" (bottom)

This was confirmed by the results of experiments carried out by Almaz-Antey Corporation specialists.<sup>89</sup>

#### Mechanical (penetration) capacity

Shell fragments, with their relatively low mass and large linear dimensions (Figure 5.2.25 above), decelerate faster in air and their impact on obstacles (penetration) under the same conditions is significantly lower than that of prefabricated projectiles. This is illustrated in more detail in Exhibit A of the Field Experiment Report (2016).<sup>90</sup>

As one illustrative example, the differences in the penetration (mechanical)

<sup>89</sup> Almaz-Antey report on the full-scale experiment (2016).

<sup>90</sup> Exhibit A to the Field Experiment Report, section 3.1, pages 17-27.

capacity of off-the-shelf and body-mounted projectiles when secured in a particularly strong "trap" barrier are shown.<sup>91</sup>

Prefabricated projectiles of all fractions, taking into account the outer skin of the trap and three layers of stopping foam, penetrated the complex combined obstacle to a depth of 400.0-450.0 mm (Figure 5.2.26).



Figure 5.2.26 - Removing a ready-made impactor from the "L. 1" trap: left - depth of penetration of a ready-made impactor into the trap; right - ready-made impactor 9H314M 1-9 stuck in the trap

Figure 5.2.27 shows the hull impactor (compartment hull fragment) extracted from the third layer of stopping foam of the heavy-duty booby trap "L.1".

This fragment penetrated the outer barrier of the trap (2.0 mm aluminium alloy sheet AMg6M), two of the three sheets of stopping foam PS-1-150 and was stopped at the boundary of the third layer.

<sup>91</sup> The trap is designed to trap debris and consists of several consecutive layers: an outer trap barrier (2.0mm aluminium alloy sheet AMg6M); three layers of stopping foam PS-1-150 with a total thickness of 260mm and a layer of boards with a total thickness of 750mm.



Figure 5.2.27 - Hull impactor (compartment hull fragment) lodged in the third layer of stopping foam PS-1-150 of trap "L.1" of the shielded target layout (31.07.2015)

The analysis of the results of the field tests confirms two important claims made by Almaz-Antey Corporation specialists:

1. At angles close to normal (shielded target conditions), aluminium barriers (similar to the outer skin of a Boeing 777) are capable of penetrating not only prefabricated projectiles but also hull fragments.

2. Ready-made projectiles provide a much more destructive effect after piercing the fuselage of any aircraft and will cause a great deal of damage to the interior of the aircraft.

Combat damage studies of the Boeing 777 show that penetrating and non-penetrating damage on the aircraft structure fragments was caused not only by prefabricated projectiles, but also by other parts of the weapon. This is especially true for the rear front of the fragmentation field (when impacted at angles close to normal).

As an example, Figure 5.2.28 shows photographs of through-and-through holes at the forward boundary of the fragmentation field on the fragment in front of the front windows of the Boeing 777 cockpit.

These photos were taken at Gilze-Rijen airbase in May 2015 and show examples of through-hull penetrations caused by hull-mounted projectiles.

That these injuries were not caused by prefabricated projectiles is confirmed by the shape, appearance and linear dimensions of the holes (Figure 5.2.28).

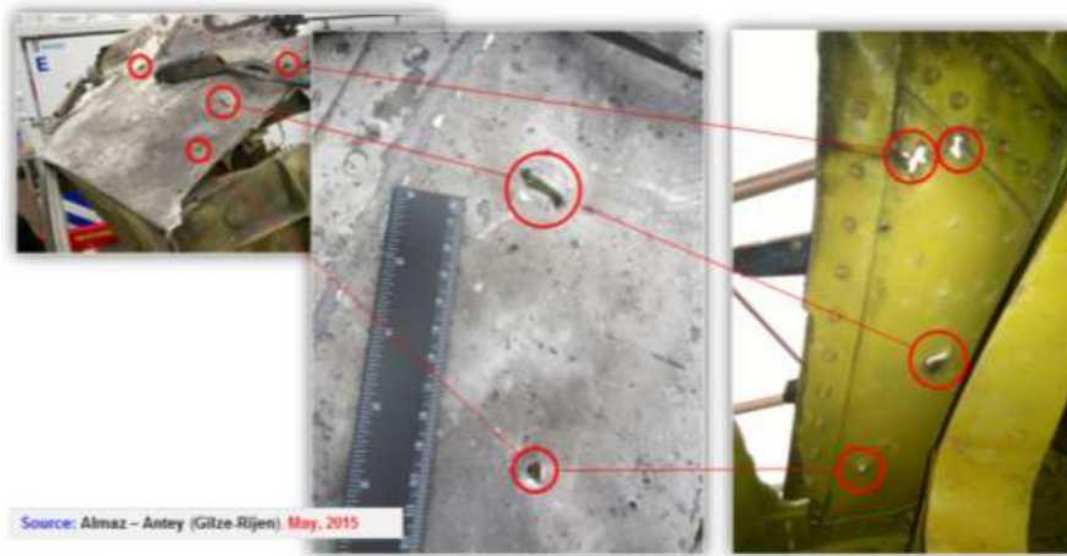


Figure 5.2.28 - Hull damage to the nose section of a Boeing 777 (external and internal view)

In this case, at small angles between the velocity vector and the plane of the obstacle, the housing fragments, unlike preformed fragments,<sup>92</sup> do not preferentially penetrate beyond the obstacle and the element ricochets without penetrating the obstacle as shown in Figure 5.2.29.



Figure 5.2.29 - At small angles between the velocity vector and the plane of the obstacle, hull fragments do not penetrate beyond the obstacle and ricochet occurs

#### Areas of high density of ready-to-use destruction elements

The presence of the maximum fragmentation field density region of the 9H314M warhead ("scalpel") and its parameters have been confirmed experimentally.

<sup>92</sup> PART 2. Exhibit B.4. Specific experimental studies to assess piercing action of ready-made projectiles.

The results of the conducted static tests confirm the formation of a dense fragment flow - the coincidence in space of the area of maximum concentration of the number of fragments with the area of their maximum velocity.<sup>93</sup> That is, the combination in space of the three most important components: the number of fragments, their total mass and velocity - the area of maximum kinetic energy of the killing field, which is called the "scalpel".

The results obtained during the second experiment allow us to conclude that when the warhead 9H314M of a BUK missile is detonated under the conditions of the DSB Report, a dense stream of projectiles penetrates the cockpit structure through. This is confirmed by the video and photographic material presented in the Corporation Report (2016)<sup>94</sup> and Exhibit B.3.

It is the "scalpel" that pierces through the structure of the aircraft and causes the most damage to the aircraft's interior.

An example of inside-out punctures on the starboard side of an IL-86 target aircraft is shown in Figure 5.2.30.



Figure 5.2.30 - Examples of through-hole exit punctures ("inside-out") on the starboard side of the IL-86 target aircraft

A dense stream of projectiles penetrating the aircraft hull successively overcome at least three to five combined dispersed obstacles in varying combinations (elements of the outer skin of the aircraft on the port side and/or roof; thermal insulation and decorative panels of the port side and/or roof; panels or cabinets of equipment on the port side or roof; cockpit floor, including longitudinal

<sup>93</sup> PART 2: Exhibit B.2.2.

<sup>94</sup> Report on the conduct of a full-scale experiment, pages75-88; 149-157. 1

or transverse force components; panels or cabinets with equipment on the starboard side or under the cockpit floor; thermal insulation and decorative panels on the starboard side or underside; elements of the external skin of the aircraft on the starboard side or underside of the aircraft).<sup>95</sup>

Also, the results of the experiment confirmed the coincidence of the calculated model of the impact of the dense flux of the preformed fragments with the actual experimental result.<sup>96</sup>

Accordingly, the use of a methodology to determine the orientation of the missile relative to the aircraft structure is justified, as the methodology has experimental validation and acceptable accuracy.

As noted in paragraph 5.1.2.9 of this report, the damage study of the Boeing 777 found that the distribution of fragmentation damage density coincides with the areas and directions of perforation and destruction of the Boeing 777 airframe, cockpit floor and the areas of "inside-out" exit fragmentation damage (Figure 5.2.31).

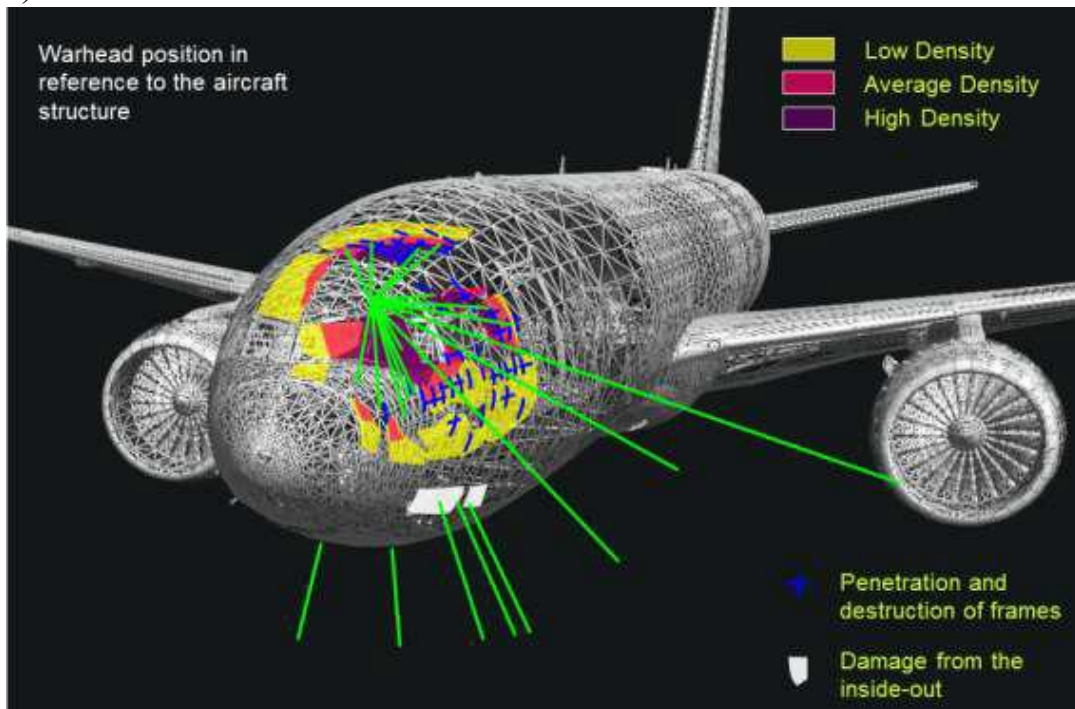


Figure 5.2.31 - Fragmentation damage density distribution coincides with the areas and directions of perforation and fracture of the Boeing 777 airframe elements

The essence of the method for determining the orientation of a missile relative to an aircraft at the moment of a warhead explosion is to find the best match between the spatial position of the dense fragmentation flow under dynamic conditions and the observed pattern of perforation and destruction of the outer hull, structure, cockpit floor and exit holes on the studied debris.

<sup>95</sup> Report on the conduct of a full-scale experiment, pages 90-107; 157.

<sup>96</sup> PART 2: Exhibit B.3, section "Piercing the Structure of the Aircraft (Target Aircraft) Through".

The result of the search is the best possible alignment of the 'scalpel' area with the damage model, taking into account the detonation point linking them.

Studies carried out by the Corporation's specialists on fragments of the roof, port side, transparency frame, cockpit floor and structure of the aircraft,<sup>97</sup> which were available for study, revealed evidence of compartment damage caused by the dense flow of debris and the resulting shock waves (aero-impact) on the Boeing 777 structure.

Exhibits A.3 and A.4 present several examples of damage corresponding to exposure to a dense fragmentation flow region where the fragmentation density was so high that the mechanical effects of the preformed fragments (number, mass, speed), together with the aerodynamic loads acting on the aircraft in flight, caused its structure to break or puncture through.

Such damage can be traced from the outside skin of the port side through the cockpit, including the floor - outwards (at the bottom of the port side).

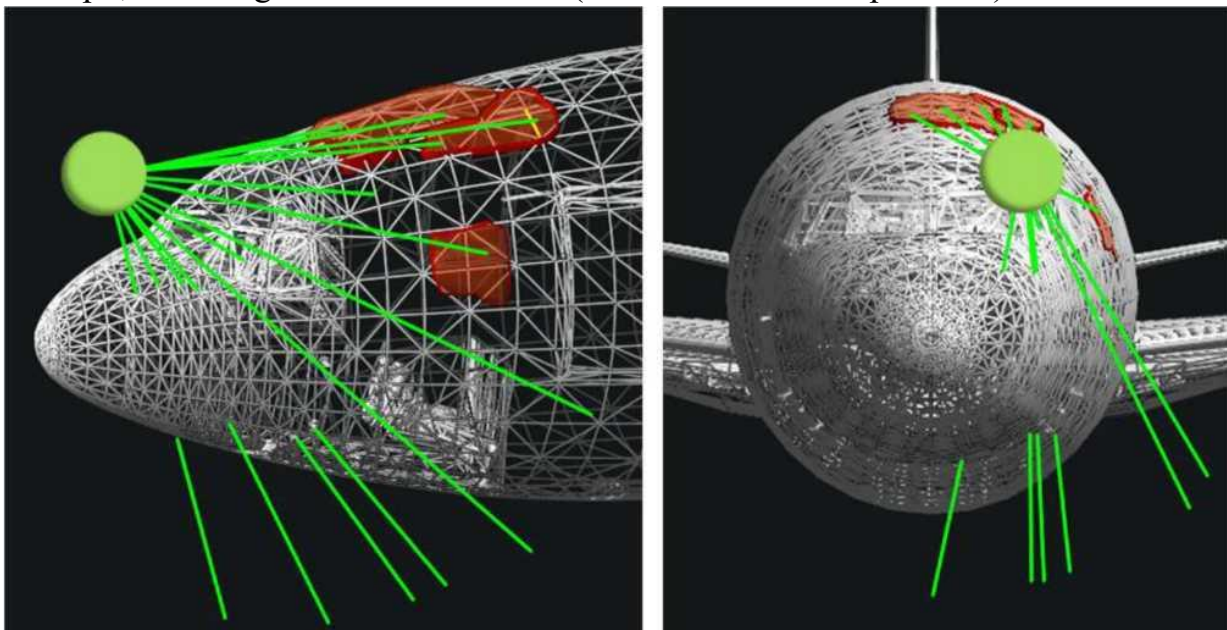


Figure 5.2.32. Visualization of approximate trajectories of ready-made projectiles in a dense fragmentation stream as it passes through or along the structure of the Boeing 777. The green ball indicates the verified detonation area, the green spokes show the directions of trajectories of preformed fragments in a dense fragmentation flow ("scalpel")

Using construction drawings and a digital model of the Boeing 777 aircraft, reference trajectories were constructed (Figure 5.2.32), which correspond to the directions of the most significant structural damage to the Boeing 777:

through-hole with exit punctures "inside-out";

penetration of two or three or more obstacles resulting in the destruction of fragments of the cockpit floor (including the transverse structural elements) along

<sup>97</sup> At the preliminary layout site in the large hangar at Gilze-Rijen airbase in February and May 2015.

the port side;

penetration of two or more barriers resulting in failure (by perforation) of the force mainframe along the left side of the roof and the port side;

Coincidence of dense fragmentation flow traces along the outer skin (ricochets) with areas of continuous failure of the bulkheads behind them.

The best results for matching the spatial position of the dense fragmentation flux with the reference trajectories were obtained for values of the horizontal angle of intersection of the missile with the aircraft's construction axis ranging from  $-66^\circ$  to  $-74^\circ$ .

Further confirmation of the range of angles of orientation of the missile relative to the aircraft (in terms of the position of the dense fragmentation stream and its effect on the aircraft structure) was obtained in the first full-scale experiment conducted under Corporation conditions - the "collision course" version.



Figure 5.2.33 - Distribution of target coverage density combined with Boeing 777 contour across the STA 220.5 level cross section

By aligning the target layout with the aircraft structure cross sections, taking into account the detonation point corrections adopted for safety conditions, confirmation was obtained that the direction of the dense fragmentation flow along the left side of the roof and the port side.

The highest fragmentation flux density is on the left side of the cockpit roof, the top and centre of the port side, the left side of the cockpit floor, as well as the area of "inside-out" exit holes at the bottom of the port side below the cockpit commander's transparency (Figure 5.2.33).

For the range of warhead orientation angles determined by this method ( $-66$  degrees to  $-74$  degrees), mapping criterion #5 (matching the nature of the damage from to the structure by dense fragmentation flow) and #8 (damage to the left wing plane and the left engine of the PTE) as specified in subsection 5.1.4 are best met.

In view of the destruction of the aircraft structure by the dense stream of projectiles ("scalpel") objectively observed on the available Boeing 777 fragments, the version that the aircraft was hit by a BUK missile can only be considered on a "collision course".

The best results for matching the missile's orientation to the aircraft at the moment of warhead detonation with the spatial position of the dense fragmentation stream are obtained for values of the horizontal angle of intersection of the missile with the aircraft's structural axis in the range of  $-66^{\circ}$  to  $-74^{\circ}$ .

#### 5.2.4.4. Matching degree of blast effect of the 9H314M warhead

Data recorded by the Boeing 777's parametric recorder at the time of its termination at 13:20:03:

height: 32,998 ft;

instrument speed: 293 knots;

magnetic heading: 115°;

drift angle: minus 4°.

Weather: wind direction: 219°;

wind speed: 36 knots;

ambient temperature: minus 44°C.

For these conditions, the effective high-explosive range of the 9H314M warhead of a BUK missile is about 3.5m.

It is known from the theory of anti-aircraft missile firing that the effectiveness of the shock wave on an airborne target depends not only on the altitude, but also on the geometric shape of the warhead, the direction of flight of the target relative to the missile and their final mutual velocity. At high missile velocities, the initial blast pressure could be two times higher than for the same explosive charge (HE) under static conditions.<sup>98</sup> The combined effect of the PM geometry and final velocity can result in a difference of more than 2.5 times in the pressure maximum of the blast wave front (depending on the direction).

Similar conclusions were reached by the Dutch experts from TNO. Annex Z of the DSB Final Report<sup>99</sup> shows the simulation calculations for a warhead detonation at an altitude of 10,000 m at a final velocity of 600 m/s.

TNO calculations show that 0.91 ms after the explosion, when the blast front reached a range of 3.0-3.3 metres, the difference in maximum pressure depending on direction is more than 2.3-2.6 times.

For example, the pressure peak in the direction perpendicular to the missile's axis (radial) is about 1,400 kPa and in the 45° downwind direction (45°) 600 kPa, which significantly affects the distribution of blast damage.

Structural damage to the Boeing 777 from near blast factors is presented in paragraph 5.1.3, which shows that deformation and fragmentation of the Boeing 777 structure (external skin and structure) has spread along the left side of the aircraft structure and reaches the level of bulkheads STA 287.5-STA 309.5. Damage along the port side has spread to more than 4 meters from the front border of damage - front hermetic bulkhead STA 132.5.

To assess the orientation of a warhead by the nature of the close blast damage, it is most important to examine the fragments closest to the point of blast and having surfaces oriented frontally to the direction of blast wave propagation.

---

<sup>98</sup> Neupokoev F.K. Anti-Aircraft Missile Firing. Pages 200-201.

<sup>99</sup> TNO Report 2015M10626. Numerical simulation of blast loading on Malaysia Airlines flight MH17 due to a warhead detonation.

Such a fragment that satisfies these requirements is the nose section of the Boeing 777, adjacent to the front bulkhead at the top (Figure 5.2.34).



Figure 5.2.34 - Fragment of the nose of a Boeing 777, adjacent to the front bulkhead from above (photo February, 2015)

There are several important facts that come to mind when assessing the blast effect:

Minor tearing of the bulkhead wall as well as the sheathing failure with deformation of the bulkhead flange to the left and below the fragment in question;

the anterior boundary of the shattered cover field runs along the rear of the fragment (shatter action is observed on transparency remnants), with no residual macro deformation of the glass and its destruction is due to shattering perforation;

No noticeable permanent deformation of the left-hand windscreen wiper close to the point of detonation;

the remaining surface of the fragment before transparency shows only clearly distinguishable traces of close blast products: microcratering, thermal oxidation and soot (Figure 5.2.35).



Figure 5.2.35 - Most of the fragment shows only clearly visible traces of close blast products: microcratification, thermal oxidation and soot (photograph February 2015)

Thus, despite the close blast (not more than 2.0 m from the fragment), the high-explosive effect on this fragment was very low and did not exceed the critical (destructive) value with respect to the fuselage front structure in the cockpit area.

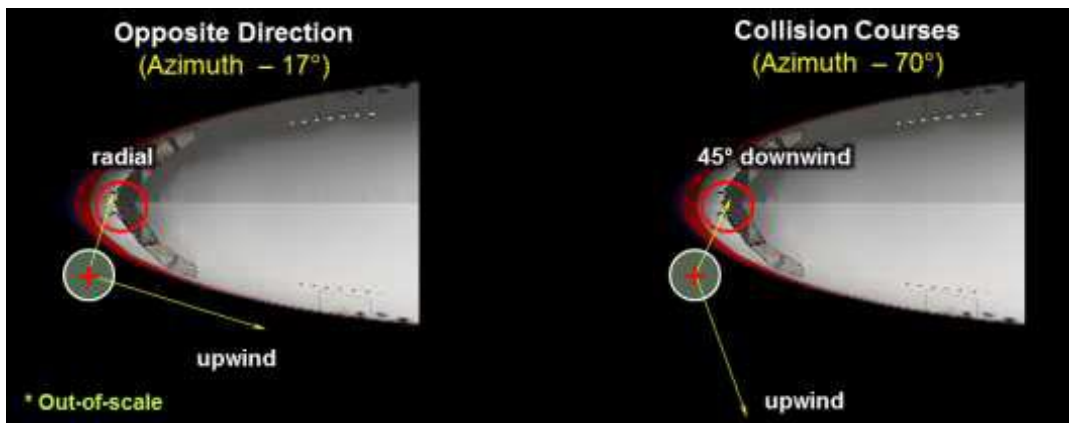


Figure 5.2.36 - Comparison of impact conditions on a fragment of Boeing 777 nose section adjacent to the front bulkhead from above: left - "on an oncoming course"; right - "on a collision course"

Figure 5.2.36 shows a diagram derived from the calculations, showing the blast wave impact directions from the verified detonation region for the two versions of the 9M38 missile impact considered.

As can be seen from the diagram, the preservation of a fragment located at a short (no more than 2.0 m) distance from the detonation point of the 9M38 warhead can only be explained for the "collision course" version.<sup>100</sup>

Calculations have shown that if the explosion occurred within 1.6-2.0 m, the most likely conditions are that the missile crosses the course of the aircraft between  $-68^\circ$  and  $-72^\circ$  (Criterion #7).

The non-compliance of the landmine impact of the basic DSB version ("opposite course") was also demonstrated in the Air Force Central Research Institute contribution to the joint work of the international expert group.<sup>101</sup>

The in-situ tests resulted in experimental confirmation of the non-compliance of the blast effect of the 9H314M warhead with the basic DSB ("opposite course") version. A comparative analysis of the damage to the IL-86 and Boeing 777 (MH17) target aircraft from close blast factors is given in Exhibit A.4.3.

The main conclusion of the studies is that the orientation of the warhead, under the conditions of the IL-86 target aircraft experiment (according to the DSB version an opposite course", i.e. about  $-17^\circ$ ), is not consistent with the spread and nature of damage to MH17 from close blast factors.

Thus, as a result of calculations confirmed by field tests, it is established that the nature of damage from close blast factors on the Boeing 777 structure is not consistent with the "opposite course" version (test results significantly exceed the level of damage observed on the MH17 fragments).

---

The angle of intersection of the longitudinal axes of the aircraft and missile in the horizontal plane at which it is possible to consider a version of aircraft damage as a result of a near missile explosion was more than  $-50^\circ$ , and the most probable conditions were that the missile crossed the aircraft course between  $-68^\circ$  and  $-72^\circ$ .

---

<sup>100</sup> PART 2: Exhibit A.4.3 Dynamic conditions, pages 50-52.

<sup>101</sup> Calculation Results of Warhead Location at the Moment of Detonation.

#### 5.2.4.5. Verification of the results obtained on the basis of in-flight control data

An analysis of the objective control materials recorded by the Utes-T air-route radar complex located at the Ust-Donetsk radar position showed that in the primary data registration file "14-07-17.kt" for the period from 13:02 to 13:32 UTC 17.07.2014, no markings from the weapon were registered. This indicates the absence of an object moving towards the Boeing 777 "on an oncoming course" (according to the DSB) in the observation space.

In order to confirm the technical characteristics of Utes-T, a full-scale experiment (flight test of the Utes-T ARRC) was conducted, approximating as closely as possible to the conditions at the time of the crash.<sup>102</sup> Main results:

1. The radar detection capability of Utes-T has been confirmed to match the radar signature of the 9M38 missile. A missile flying at altitudes above the radio horizon can be detected by the primary radar at ranges greater than 200 km.

2. Utes-T 's ability to detect and track supersonic objects without interference has been confirmed (Figure 5.2.37).

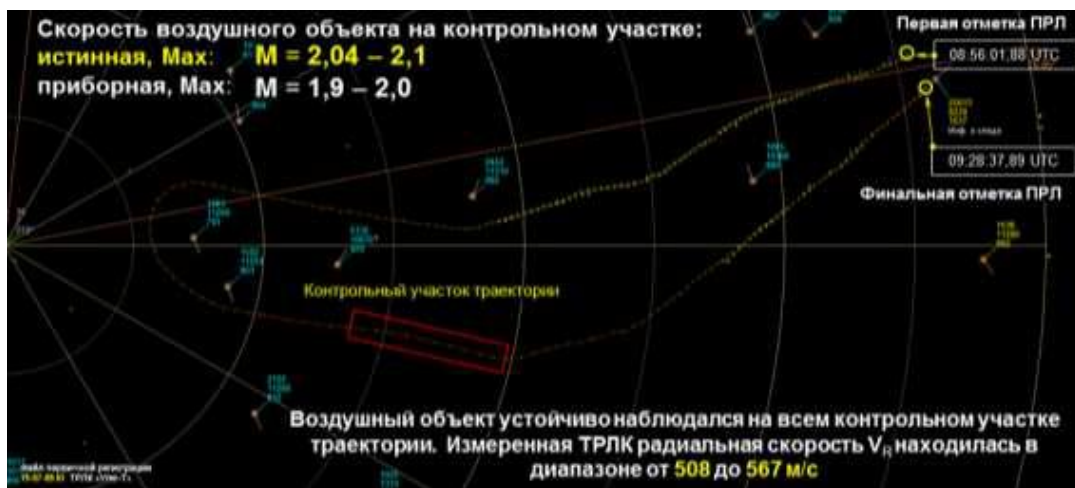


Figure 5.2.37 - Supersonic Air Object Escort

3. The conditions under which the absence of primary marks from the missile in the logging file is possible have been theoretically determined and practically confirmed during a series of overflights.

The main conclusion: the unregistered radar-guided BUK missile **could only approach the Boeing 777 from a southerly direction - "on a collision course"**, which rules out collision course angles in the horizontal plane of less than  $-60^\circ$ .

<sup>102</sup> Report "On conducting a flight check of the Utes-T track radar complex located at the Ust-Donetsk track radar position of the Rostov zonal centre of the Unified Air Traffic Management System of the Russian Federation", 2019.